electronics

MDPI

Article

Is the Neuromuscular Organization of Throwing Unchanged in Virtual Reality? Implications for Upper Limb Rehabilitation

Emilia Scalona [1,2,†], Juri Taborri [3,*,†], Darren Richard Hayes [1,4], Zaccaria Del Prete [1], Stefano Rossi [3] and Eduardo Palermo [1]

[1] Department of Mechanical and Aerospace Engineering (DIMA), Sapienza University of Rome, 00185 Roma, Italy; emilia.scalona@in.cnr.it (E.S.); dhayes@pace.edu (D.R.H.); zaccaria.delprete@uniroma1.it (Z.D.P.); eduardo.palermo@uniroma1.it (E.P.)

[2] National Research Council (CNR), Institute of Neuroscience, 43125 Parma, Italy

[3] Department of Economics, Engineering, Society and Business Organization (DEIM), University of Tuscia, 01100 Viterbo, Italy; stefano.rossi@unitus.it

[4] Seidenberg School of CSIS, Pace University, New York, NY 10038, USA

* Correspondence: juri.taborri@unitus.it; Tel.: +39-076-135-7049

† These authors contributed equally to this work.

Received: 6 November 2019; Accepted: 4 December 2019; Published: 6 December 2019

Abstract: Virtual reality (VR) is an appealing approach for increasing the engagement and attention of patients during rehabilitation. Understanding how motor control changes in real vs. virtual scenarios is a research challenge in terms of validating its administration. This study evaluates muscle synergies when subjects conduct throwing tasks in virtual reality. Seventeen healthy subjects performed 20 throws both in a virtual environment and in real one as they threw a ball with both dominant and nondominant arms. The electromyography (EMG) signals of 11 muscles of the upper limbs were recorded. Non-negative matrix factorization was used to extract muscle synergies. The cosine similarity was computed to assess the consistence of muscle synergy organization between virtual and real tasks. The same parameter was used to establish the inter-subject similarity. A three-synergy model was selected as the most likely. No effects of virtual reality and arm side on neuromuscular organization were found. Forearm muscles, not necessary for ball holding and release, were comprised in the activation synergies in the virtual reality environment. Finally, the synergies were consistent across subjects, especially during the deceleration phase. Results are encouraging for the application of virtual reality to complement conventional therapy, improve engagement, and facilitate objective measurements of pathology progression.

Keywords: muscle synergies; virtual reality; throwing; muscle activation; rehabilitation; upper limb

1. Introduction

Virtual reality (VR) is a tool for replicating or augmenting real environments with varying levels of involvement [1]. Immersive virtual reality provides a more comprehensive sensing experience, by leveraging interface tools such as a video headset [2], or devices for delivering tactile information [3]. A non-immersive version, whereby the visual interface is a computer screen, is generally easier and faster to implement [4]. The natural engagement of subjects with VR has fueled its adoption beyond gaming, making VR-based solutions available for a wide range of experiences, ranging from education to physical rehabilitation [5,6].

Physical rehabilitation is used to facilitate the recovery of patient impairments linked to injury or pathology. Considering incidents that cause damage to the central nervous system (CNS), including stroke, or neurodegenerative diseases, such as Parkinson's, it is critical to understand the

importance of the research related to effective solutions for motor rehabilitation. Stroke, for instance, affects about 10 million people every year [7], often causing the demise of brain cells in the motor cortex area, resulting in the inability to perform typical daily-life gestures. Motor rehabilitation should be initiated, during the so called "sub-acute" phase, to administer structured exercises involving physical interaction within an environment, thereby fostering motor re-learning [8].

After the subacute phase, where patients experience a rapid recovery to realize much of their original abilities, they enter the chronic phase, which is characterized by a stabilized damaged tissue condition, and a slower rate of recovery from motor impairment [9]. Regarding those who suffer from neurodegenerative diseases, during this phase, patients often experience a lack of motivation, which may lead to them dropping out of a rehabilitation program [10]. Over the past decade, portable and low-cost solutions for introducing rehabilitation into a domestic environment have been investigated [11,12]. These solutions, derived from robot-mediated therapy (RMT) [13], involve simple devices, thereby rendering them suitable for the chronic stage, where assistive mechanical power might be not be needed. The ability to move a rehabilitation program to a domestic environment is expected to encourage participation in the program [14]. In supporting this goal, VR is often leveraged in this context to increase motivation and engagement [15,16]. Scalona et al. proposed a protocol for the evaluation of motor learning in a 3D space using a low-cost haptic device in a VR environment [17]. Summa et al. [12] designed VR-based upper limb training for PD patients, which involved 3D arm gestures, to decrease bradykinesia. Pastor et al. [18] used a computer game to facilitate the rehabilitation of stroke survivors, while Laut et al. [19] tested the efficacy of navigating a virtual environment to evaluate and train the motor performance of children with cerebral palsy (CP).

The general paradigm of these solutions is the interaction with VR through a physical device, such as haptic joysticks [19,20] and/or motion trackers [21]. In the latter category, Microsoft Kinect has been used in experiments as a low-cost markerless solution for human motion tracking [22,23], as it offers a tremendous potential to serve as a natural user interface [24]. As a result, the number of proposed solutions for portable rehabilitation protocols, leveraging the Microsoft Kinect and VR, has rapidly increased [25]. In some cases, the same kinematic indices of performance, introduced in RMT and in kinematic evaluations based on optoelectronic systems (OS), were implemented on data obtained through the Kinect, as an assessment tool for motor control abilities [26].

However, although real and VR motor tasks can be considered equivalent in terms of kinematics, the pattern of induced muscular activation in these two scenarios may be different. Sabatini [27] demonstrated that a cohort of healthy subjects exhibited different patterns of muscle movement while performing the same reaching task with the upper limb. These differences were more evident when analyzing electromyography (EMG) signals than kinematic data, thereby demonstrating a potential difference in the internal feedforward motor command of subjects. On the other hand, Kang et al. compared the muscle activity with fully immersive VR to real archery motions in order to investigate the effects of VR. The authors found no significant difference between real and virtual tasks in terms of muscle activity patterns [28]. These findings encouraged us to question whether virtual reality can be used for rehabilitation, thereby studying different muscle activation by means of muscle synergies.

According to the muscle synergies theory, the EMG-enveloped profiles of a set of muscles involved in a complex coordination task can be represented as the linear combination of a reduced number of command signals, known as motor primitives (or factors) with a corresponding weight for each muscle [29]. This factorization can represent a coordinating activation of different muscles, during the different phases of a gesture, in a space of reduced dimensionality [30]. This theory was initially applied to repetitive and automated gesture, such as gait [31–34] and balance adjustments [35–37]; since then, several applications in clinics, sports, and robotics have been proposed [38]. Repetitive movements, such as gait, although complex, are highly automated in normally developed subjects and, thus, imply a reduced activation in the motor cortex area with respect to upper limb gestures. Several studies have demonstrated consistency in factorization parameters (motor primitives and weights vectors) across groups of subjects performing the same task, thereby supporting the hypothesis that those factors might represent internal strategies that the central nervous system (CNS) adopts for managing the complexity of motor coordination [32,39–42].

Although the transfer of these techniques from lower limb tasks to upper limb ones is difficult, due to a greater variety and complexity of upper limb gestures [43], an analysis of muscle synergies still represents a consistent method for evaluating the coordination of muscle activation. In reference to throwing, Cruz-Ruiz and colleagues showed that three muscle synergies were sufficient to reconstruct the EMG data relating to overhead football throws [44]. However, to the best of authors' knowledge, no studies have been conducted to evaluate the muscular organization in Virtual Reality environments during repetitive tasks. Thus, it could also be leveraged to evaluate the similarity of VR-based vs. real tasks in rehabilitation, in terms of the similarity in muscle activation. The aim of this study is the validation of a typical VR-based upper limb rehabilitation gesture in terms of muscle activation. In particular, we sought to evaluate whether a VR task, replicating throwing a ball, can elicit a similar level of muscle synergies involved with a real throwing task. The throwing task was selected as a gesture involving the coordinated activation of different muscles to move the upper limb against gravity, and therefore represents a specific, yet paradigmatic, gesture for home VR-based rehabilitation. An additional goal was to evaluate the inter-subject similarity in muscle synergy organization when subjects with a comparable health status are asked to perform a throwing task, while gaining an understanding of the role of each synergy in the throwing phases. The outcomes of this study could prove to be useful when implementing rehabilitative protocols, based on VR, thereby potentially encouraging adherence and adaptability to rehabilitation programs, while quantifying performance.

2. Materials and Methods

2.1. Experimental Setup

The experimental setup consisted of a laptop, where the non-immersive VR scenario was implemented, a Microsoft Kinect 2.0 sensor, for interacting with the VR, and a 16-channel wireless EMG system (Cometa Zero Wire, Milan, Italy).

The VR scenario was developed in the Unity 3D game engine and it is reported in Figure 1. It consists of an essential three-dimensional environment, which is comprised of a green floor separated on the horizon by a blue background. The virtual object to be thrown has the shape and size of a ball, while a wooden barrel is used as the target to hit. To make the ball appear on the screen, the player has to raise their arm. Once the ball appears at the bottom of the screen, the subject can proceed with a throwing motion that is reproduced by the Kinect sensors with the movement of the ball on the screen. The speed of the ball is proportional to the hand movement speed. A counter at the top left of the screen returns the number of successful launches (ball–barrel collision), thereby providing immediate feedback on user performance.

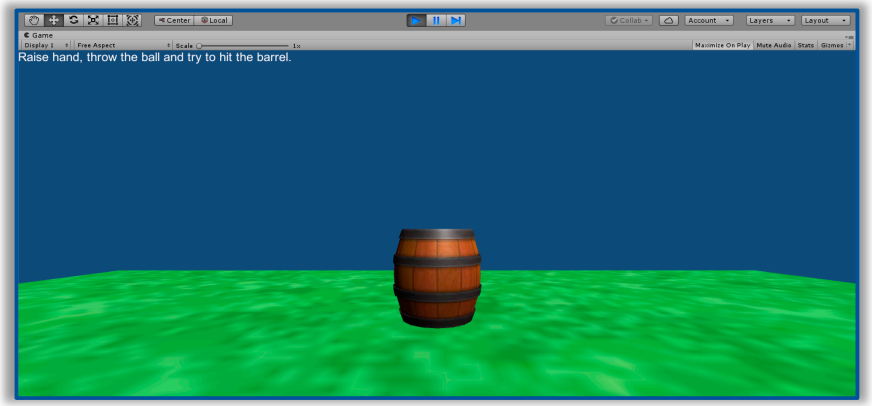

Figure 1. Game scenario developed in Unity 3D.

2.2. Experimental Protocol

Seventeen subjects (nine males, eight females, aged 25 ± 4) with no history of injuries or pathologies to the upper limbs were enrolled in the study. Fifteen out of the seventeen subjects were right-handed.

Each subject was instrumented with EMG probes on 11 muscles of a side, as reported in Figure 2, to record the muscle activity during the experimental tasks.

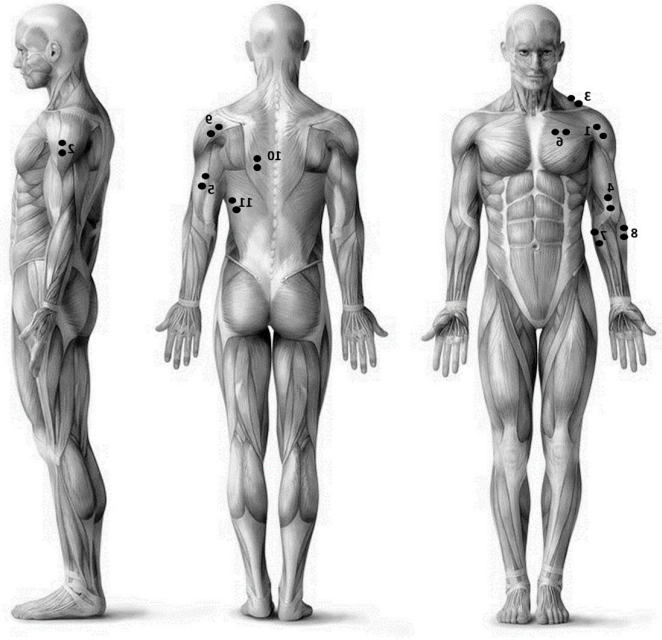

Figure 2. Electrode placements: (1) Deltoideus Anterior (DeltA); (2) Deltoideus Medius (DeltM); (3) Trapezius Descens (TrapD); (4) Biceps Brachii (BB); (5) Triceps Brachii long head (TBL); (6) Pectoralis Major (PM); (7) Flexor Carpi Ulnaris (FCU); (8) Brachioradialis (BRD); (9) Deltoideus Posterior (DeltP); (10) Trapezius Trasversalis (TrapT); (11) Latissimus (Lat).

In order to minimize the impedance due to skin and sweating, the selected areas were initially rubbed with alcohol. Electrodes were then placed in accordance with the placement guidelines of the European project SENIAM (surface electromyography for the noninvasive assessment of muscles) [45].

Each subject was asked to perform two throwing tasks. The first task consisted of throwing a virtual ball within the Unity 3D platform: the movement began with the arm raised and ended in a position of rest, which was with the arm parallel to the body, and recorded for a total duration of 5 seconds. The distance of the subjects from the computer was 2 meters. The second task required a throwing motion with a ball (diameter 6.5 cm, weight 30 g) against the wall, where a representation of the barrel was positioned. The distance from the target remained unchanged with respect to the virtual task. The two tasks were performed with both the dominant and nondominant arm. The dominant arm was selected as the one commonly used, by the participant, for writing. For each task, 20 launches were performed for a total of 80 launches. Before proceeding with the tests, a reference electromyographic signal, addressed as baseline, was recorded with the subject in the rest position, guaranteeing that there was no muscle activation. The order of four tasks was randomized across the subjects to avoid bias in the data due to the same task sequence. In order to avoid a visual familiarization with the task, each subject was tested individually. The entire protocol lasted approximately 30 minutes per subject.

The research was approved by the local ethical committee (Sapienza University of Rome) and it was conducted according to the principles expressed in the Declaration of Helsinki. Written informed consent was obtained from each participant.

Figure 3 depicts a subject with EMG probes performed both the real task and the virtual one.

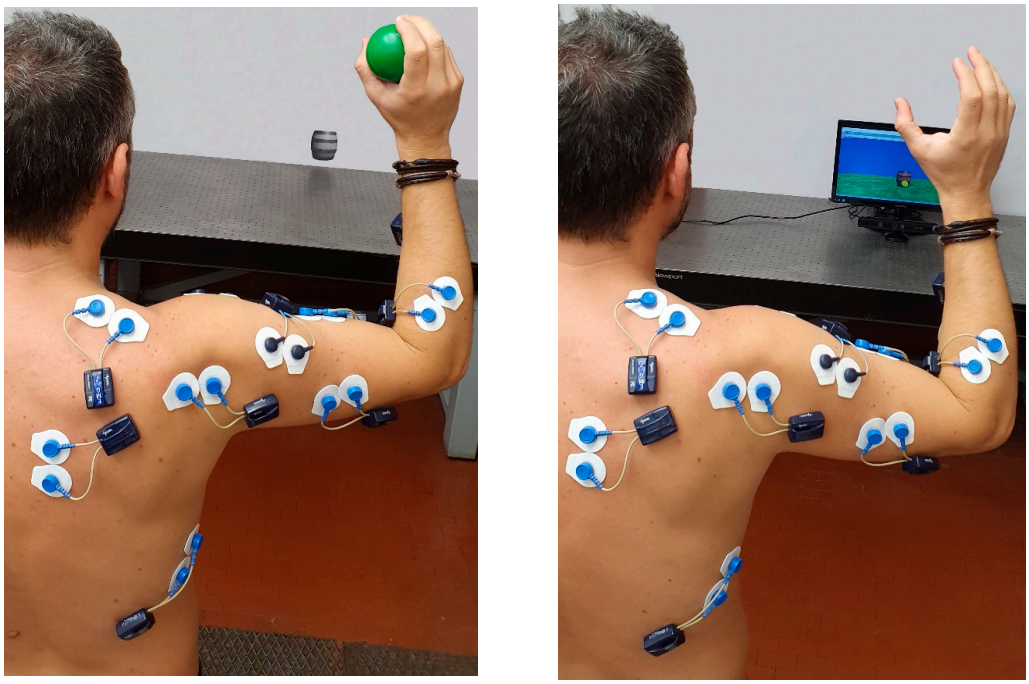

(a) **(b)**

Figure 3. A subject with electromyography (EMG) electrodes performing both the real task (**a**) and the virtual task (**b**).

2.3. Data Processing

For the purposes of extracting muscle synergies, the recorded electromyographic signals were processed by conventional filtering and grinding methods [44,46] implemented in MATLAB (R2014a, MathWorks, Natick, MA, USA, 2014). In particular, the baseline was removed from the raw signals, and then filtered. A fourth-order Butterworth low-pass filter with cutoff frequency equal to 450 Hz was applied to outline the upper limit of the band of interest. The same filter, but in high-pass mode with a cut-off at 10 Hz, allowed the elimination of noise at low frequencies and the continuous residual component. A Notch filter centered at 50 Hz removed the power network component. Then, the signal was rectified, and an additional fourth-order Butterworth filter was applied in a step-by-step mode with a cut-off frequency of 6 Hz to extract the envelope.

Subsequently, each EMG signal was resampled at 1000 samples in order to normalize the duration of a single throw. The amplitude of each EMG vector was normalized with respect to the maximum activation, defined as the maximum value across all repetitions and all tasks. Finally, the 20 signals of each repetition related to the task were concatenated one after the other, attaining an EMG matrix ($m \times n$) for each subject and each task by grouping the n-sample signals of the m considered muscles by row. For each experimental condition, m was equal to 11 and n was equal to 20,000, that is 20 launches × 1000 frames.

The matrix obtained was used as the input of the non-negative matrix factorization (NNMF) algorithm for the extraction of the muscle synergies. NNMF was selected among other factorization algorithms because it provides the most reliable outputs [32]. The algorithm allowed us to compute the muscle synergy vectors (W_i) and the temporal activity patterns (C_i), as a linear combination reported in Equation (1) [47]:

$$\boldsymbol{EMG} = \sum_{i=1}^{s} W_i C_i + \varepsilon;\ s \leq m \quad (1)$$

where s corresponds to the number of muscle synergies and ε represents the difference between the acquired EMG matrix and the reconstructed one. The reconstructed EMG was obtained by applying the linear combination of W_i and C_i in the output of NNMF. The muscle synergy vector W_i is independent of time and it is composed of only positive weights, indicating the involvement of each muscle in the i-th synergy. Instead, the temporal activity pattern C_i is a time-dependent waveform, considered as a representation of the neural command for the activation of the i-th synergy. The following parameters were set: 50 replicates and 1000 maximum iterations for minimizing the squared residual between acquired and reconstructed signals [48]. We performed the computation 11 times, with the s value ranging from 1 to 11. Figure 4 shows a schematic explanation of the muscle synergy theory.

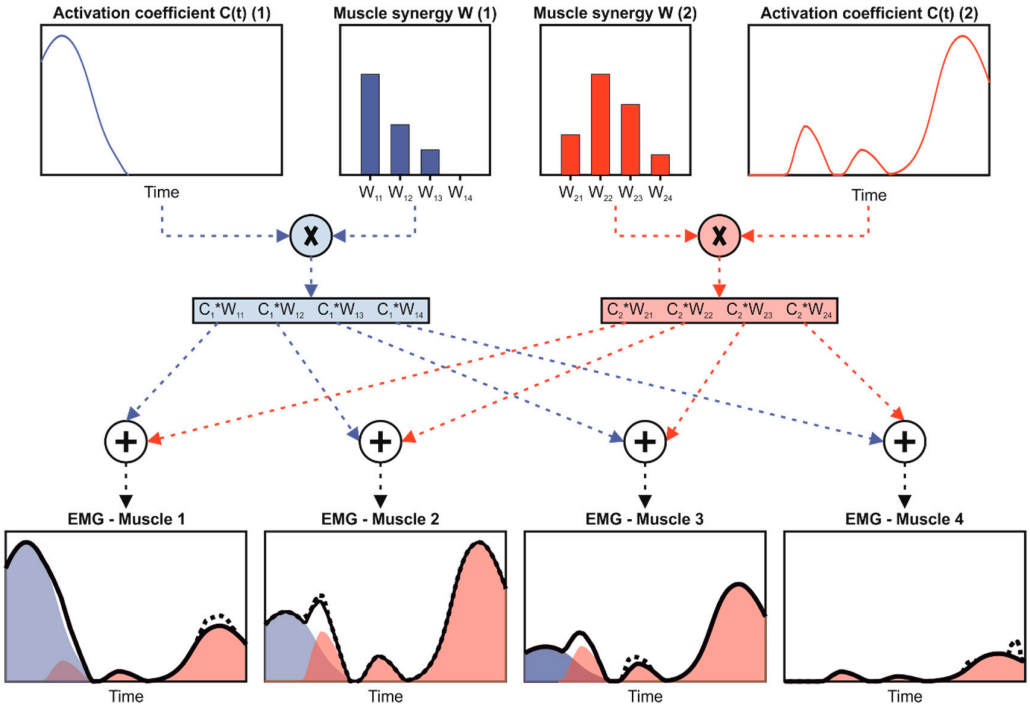

Figure 4. Schematic explanation of muscle synergy theory. Reconstruction of four muscles with the linear combination of two muscle synergies (blue and red).

2.4. Data Analysis

When selecting the minimum number of muscle synergies (NoS), we used variability account for (VAF) index. This index allowed us to assess the similarity between the acquired and reconstructed EMG signals [39] and it is computed as the uncentered Pearson's coefficient, expressed as a percentage between the two signals. Pearson's coefficient allowed us to quantify the linear correlation between two vectors [49]. Two different VAFs were computed for the selection of NoS: the first one, named global VAF (VAF_{glo}), was calculated between the acquired and the reconstructed EMG matrices, while the second one, named local VAF (VAF_{loc}), was calculated between the acquired and the reconstructed EMG signals of each muscle. VAF_{glo} and VAF_{loc} were calculated for all of the tested s values. Finally, for each subject and each task, NoS was selected as the model with the minimum number of synergies that simultaneously met the two selection criteria: $VAF_{glo} \geq 90\%$ and $VAF_{loc} \geq 75\%$ [39,50]. Thus, the NoS represents the minimum number of synergies required to obtain a proper representation of the muscle activation data by using the linear combination in Equation (1). Then, the mode of NoS across all of the four examined tasks was selected individually for each subject and the respective model was considered for analysis. It should be noted that the model with the lower number of muscle synergies was used for the successive analyses when more than one muscle synergy model had the same number of occurrences for the examined subject. As it is well-known

that the order of synergies in the model is not consistent among different runs of the NNMF algorithm [48], we performed a K-means cluster analysis to select and to order similar synergies among tasks, individually for each subject [51]. In particular, the most correlated synergy vectors that fell within one cluster according to the K-means outputs were considered related to the same *i*-th synergy in the selected model among tasks. Successively, individually for each subject, we evaluated the robustness of the muscle synergy vectors among the four tasks by computing the cosine similarity (cos_{sim}), which is defined according to Equation (2) [32]:

$$\cos_{sim}(\mathbf{W}_x, \mathbf{W}_y) = \frac{\mathbf{W}_x \cdot \mathbf{W}_y}{\|\mathbf{W}_x\| \|\mathbf{W}_y\|} \quad (2)$$

where $\mathbf{W}_x$ and $\mathbf{W}_y$ represent the pair of tested $\mathbf{W}s$ in turn. This index can assume values ranging from 0 to 1, corresponding to no- and perfect similarity, respectively. The threshold value for cos_{sim} to assume similarity was set to 0.60 [52]. Thus, we performed four comparisons: (i) VR-based task vs. real task performed with the dominant arm—$^{VR/R}CS_D$; (ii) VR-based task vs. real task performed with the nondominant arm—$^{VR/R}CS_{ND}$; (iii) dominant vs. nondominant arm in performing VR-based tasks—$^{D/ND}CS_{VR}$; and, (iv) dominant vs. nondominant arm in performing real tasks—$^{D/ND}CS_R$. Comparisons were obtained individually for each subject and each synergy in the selected model. In addition, the similarity of the overall selected model, i.e., considering all of the *i*-th synergies together, was computed by independently averaging the obtained cos_{sim} for each synergy in the model, individually for each subject and each task. This similarity analysis allows a comparison of the muscle synergy organization when performing throwing tasks in VR environments and as a real task with both the dominant and nondominant arm.

When assessing the similarity across all subjects in performing the same task, the most common model found considering all the examined tasks and all the subjects together was selected. Then, after a new application of k-means analysis for the reorder, the cos_{sim} index was computed for each task. We performed 136 comparisons, i.e., 17 subjects, for each task and each synergy in the selected model. Then, the mean and SD of cos_{sim} across the comparisons were computed to quantify the robustness of the muscle synergy vectors $\mathbf{W}$ in same task performed by different subjects.

2.5. Statistical Analysis

All data, with the exception of the NoS, were tested for normality with the Shapiro–Wilk test and the results showed a normal distribution. For all the following tests, a significance level equal to 0.05 was set. Statistical analysis was conducted using SPSS software package (v17.0, IBM-SPSS Inc. NY, USA, 2015).

A two-way Friedman's nonparametric test was performed to evaluate statistical differences in the NoS, considering the tasks (virtual vs. real) and the side (dominant vs. nondominant), as the independent variables.

To verify whether the similarity in the overall model obtained in the comparison between virtual reality task and real one was influenced by dominance in the side, a t-test was performed to compare $^{VR/R}CS_D$ and $^{VR/R}CS_{ND}$ related to the overall model. Moreover, another t-test was performed on $^{D/ND}CS_{VR}$ and $^{D/ND}CS_R$ related to the overall model to investigate if the similarity obtained in the comparison between dominant and nondominant arm is influenced by the task.

Finally, the influence of the *i*th synergy on the cos_{sim} values obtained in the between-subject analysis was tested through one-way ANOVAs, independently for each task. This test evaluates whether the similarity across subjects depends on the specific synergy in the model. When statistical differences were observed, a Bonferroni's test for multiple comparisons was performed.

For technical details about the statistical tests performed, please see [49].

3. Results

The NoS values for each task and the computed modes for each subject are reported in Table 1.

Table 1. Number of muscle synergies (NoS) for each task and each subject and mode across tasks related to each subject. D and ND stand for dominant and nondominant, respectively.

ID	VR Task		Real Task		*Mode*
	D	ND	D	ND	
ID1	3	3	3	2	*3*
ID2	3	3	4	3	*3*
ID3	3	3	2	3	*3*
ID4	3	4	3	3	*3*
ID5	3	4	3	3	*3*
ID6	3	3	3	3	*3*
ID7	3	2	2	4	*2*
ID8	2	2	3	2	*2*
ID9	2	3	3	3	*3*
ID10	4	3	2	3	*3*
ID11	2	2	3	2	*2*
ID12	3	4	3	4	*3*
ID13	4	4	3	3	*3*
ID14	3	3	3	3	*3*
ID15	2	3	3	3	*3*
ID16	3	4	3	3	*3*
ID17	4	5	4	4	*4*

Considering all of the subjects and all of the tasks, the NoS ranged from 2 to 5. Only one subject (ID14) selected the same number of muscle synergies in the four examined tasks. Considering each subject individually, the NoS mode was equal to 3 for thirteen out of seventeen subjects, while the remaining four showed a mode equal to 2 and 4, in three cases and one case, respectively. No differences were found with the statistical analysis on the median value of NoS as a function of both the task and the side ($p = 0.58$).

The results of the similarity analysis among the different tasks are reported in Tables 2–5.

Table 2. ${}^{VR/R}CS_D$ values of the similarity analysis for each subject related to the *i*-th synergy in the model, and the overall model, for the comparison: real task (R) vs. virtual task (VR), performed with the dominant side (D). Grey cells indicate value under the similarity threshold.

Real Task vs. Virtual Task—Dominant Side					
ID	**I-sy**	**II-sy**	**III-sy**	**IV-sy**	***Overall Model***
ID1	0.95	0.91	0.95	-	*0.94*
ID2	0.84	0.58	0.84	-	*0.75*
ID3	0.91	0.93	0.98	-	*0.94*
ID4	0.97	0.81	0.93	-	*0.91*
ID5	0.90	0.85	0.92	-	*0.89*
ID6	0.86	0.96	0.95	-	*0.93*
ID7	0.84	0.67	-	-	*0.75*
ID8	0.93	0.94	-	-	*0.93*
ID9	0.71	0.71	0.88	-	*0.77*
ID10	0.84	0.89	0.97	-	*0.90*
ID11	0.98	0.85	-	-	*0.91*
ID12	0.96	0.96	0.84	-	*0.92*
ID13	0.93	0.85	0.94	-	*0.90*
ID14	0.88	0.84	0.77	-	*0.83*

ID15	0.72	0.86	0.56	-	*0.71*
ID16	0.96	0.96	0.90	-	*0.94*
ID17	0.95	0.97	0.70	0.57	*0.80*

When comparing the real task vs. virtual task performed with the dominant side, the cos_{sim} was always above the similarity threshold, with the exception of three cases. In particular, values ranged from 0.56, which is the value obtained in the III-synergy for ID15, to 0.98, which is the value obtained in the I-synergy for ID11. The similarity of the overall model ranged from 0.71 to 0.94 and it was always above the similarity threshold.

Table 3. $^{VR/R}CS_{ND}$ values of the similarity analysis for each subject related to the *i*-th synergy in the model, and the overall model, for the comparison: real task (R) vs. virtual task (VR), performed with the nondominant side (ND). Grey cells indicate values under the similarity threshold.

Real Task vs. Virtual Task—Nondominant Side					
ID	**I-sy**	**II-sy**	**III-sy**	**IV-sy**	***Overall Model***
ID1	0.96	0.88	0.84	-	*0.89*
ID2	0.98	0.90	0.94	-	*0.94*
ID3	0.88	0.80	0.50	-	*0.72*
ID4	0.81	0.93	0.85	-	*0.86*
ID5	0.87	0.87	0.60	-	*0.78*
ID6	0.85	0.64	0.98	-	*0.82*
ID7	0.77	0.80	-	-	*0.79*
ID8	0.98	0.95	-	-	*0.96*
ID9	0.88	0.90	0.93	-	*0.90*
ID10	0.95	0.93	0.98	-	*0.95*
ID11	0.96	0.84	-	-	*0.90*
ID12	0.98	0.98	0.98	-	*0.98*
ID13	0.61	0.96	0.85	-	*0.80*
ID14	0.93	0.73	0.67	-	*0.77*
ID15	0.89	0.99	0.96	-	*0.95*
ID16	0.74	0.92	0.73	-	*0.79*
ID17	0.65	0.89	0.99	0.75	*0.82*

When comparing the real task vs. virtual task performed with the nondominant side, the cos_{sim} was always above the similarity threshold, with the exception of one case. In particular, values ranged from 0.50, which is the value obtained in the III-synergy for ID3, to 0.99, which is the value obtained in the II-synergy for ID15 and III-synergy for ID17. The similarity of the overall model ranged from 0.72 to 0.98, and it was always above the similarity threshold.

Table 4. $^{D/ND}CS_{VR}$ value of the similarity analysis for each subject related to the *i*-th synergy in the model and the overall model for the comparison: dominant (D) vs. nondominant (ND) side used to perform the virtual task (VR). Grey cells indicate value under the similarity threshold.

Dominant vs. Nondominant Side—Virtual Task					
ID	**I-sy**	**II-sy**	**III-sy**	**IV-sy**	***Overall Model***
ID1	0.94	0.90	0.93	-	*0.92*
ID2	0.78	0.87	0.67	-	*0.78*
ID3	0.76	0.86	0.88	-	*0.83*
ID4	0.90	0.84	0.59	-	*0.78*
ID5	0.97	0.95	0.86	-	*0.93*
ID6	0.81	0.58	0.97	-	*0.79*
ID7	0.79	0.73	-	-	*0.76*
ID8	0.91	0.85	-	-	*0.88*
ID9	0.80	0.41	0.91	-	*0.71*
ID10	0.52	0.80	0.98	-	*0.76*
ID11	0.99	0.94	-	-	*0.96*
ID12	0.93	0.92	0.83	-	*0.89*
ID13	0.74	0.84	0.95	-	*0.84*
ID14	0.77	0.91	0.92	-	*0.87*
ID15	0.73	0.91	0.89	-	*0.84*
ID16	0.55	0.81	0.83	-	*0.73*
ID17	0.74	0.82	0.58	0.94	*0.77*

When comparing the dominant vs. nondominant side in performing the virtual task, the cos_{sim} was always above the similarity threshold in all but six cases. In particular, the values ranged from 0.41, which is the value obtained in the II-synergy for ID9, to 0.99, which is the value obtained in the I-synergy for ID11. The similarity of the overall model ranged from 0.71 to 0.96, and it was always above the similarity threshold.

Table 5. $^{D/ND}CS_{R}$ value of the similarity analysis for each subject related to the *i*-th synergy in the model and the overall model for the comparison: dominant (D) vs. nondominant (ND) side used to perform the real task (R). Grey cells indicate values under the similarity threshold.

Dominant vs. Nondominant Side—Real Task					
ID	**I-sy**	**II-sy**	**III-sy**	**IV-sy**	***Overall Model***
ID1	0.91	0.82	0.81	-	*0.85*
ID2	0.74	0.87	0.71	-	*0.77*
ID3	0.85	0.90	0.69	-	*0.81*
ID4	0.94	0.67	0.47	-	*0.69*
ID5	0.92	0.82	0.61	-	*0.78*
ID6	0.91	0.88	0.97	-	*0.92*
ID7	0.78	0.51	-	-	*0.64*
ID8	0.87	0.84	-	-	*0.85*
ID9	0.89	0.53	0.98	-	*0.80*
ID10	0.90	0.96	0.98	-	*0.94*
ID11	0.96	0.80	-	-	*0.88*
ID12	0.99	0.97	0.91	-	*0.96*
ID13	0.68	0.74	0.92	-	*0.78*
ID14	0.72	0.86	0.56	-	*0.71*
ID15	0.85	0.92	0.94	-	*0.90*
ID16	0.89	0.89	0.71	-	*0.83*
ID17	0.79	0.92	0.94	0.75	*0.85*

When comparing dominant vs. nondominant side in performing the real task, the cos_{sim} was always above the similarity threshold in all but four cases. In particular, the values ranged from 0.47,

which is the value obtained in the III-synergy for ID4, to 0.99, which is the value obtained in the I-synergy for ID12. The similarity of the overall model ranged from 0.64 to 0.96, and it was always above the similarity threshold.

No statistical differences were found among the similarity obtained for the overall model in all of the four performed comparisons: (i) VR-based task vs. real task performed with the dominant arm; (ii) VR-based task vs. real task performed with the nondominant arm; (iii) dominant vs. nondominant arm in performing VR-based tasks; and, (iv) dominant vs. nondominant arm in performing real tasks.

Finally, the most common model that was selected, considering all of the subjects, was the one with three synergies, and it was used for between-subject analysis. Additionally, the similarity was assessed only with data gathered from the dominant side; moreover, as previously mentioned, no differences were found between the two sides of the upper limb. To clarify the composition of the muscle synergy vectors, Figure 5 shows the mean values for the **W** when considering all of the subjects for the three-synergy model in both the real and the virtual task.

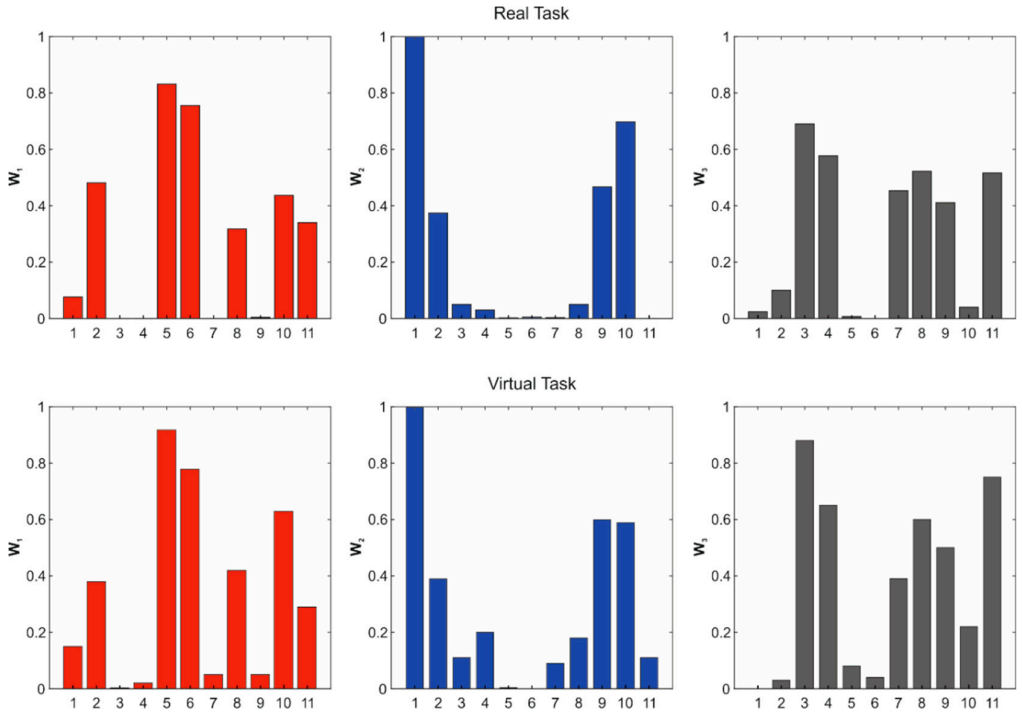

Figure 5. Mean value of muscle synergy vectors in the three-synergy model related to the real task and the virtual task. The mean was realized by averaging across subjects the muscle synergy vector. For visualization purposes, muscle synergy vectors are normalized to unity. Muscle numbers: 1: DeltM; 2: TrapD; 3: TBL; 4: PM; 5: FCU; 6: BRD; 7: DeltP; 8: TrapT; 9: LAT; 10: BB; 11: DeltA.

Mean values and standard deviations of between-subject similarity regarding the three-synergies model are reported in Figure 6. The mean value was always above the similarity threshold of 0.60. Statistical differences between the second synergy in the model (II) and the other two ($p < 0.01$) were found for the VR task, while the similarity related to the third synergy is different from the other two in the real task ($p = 0.01$).

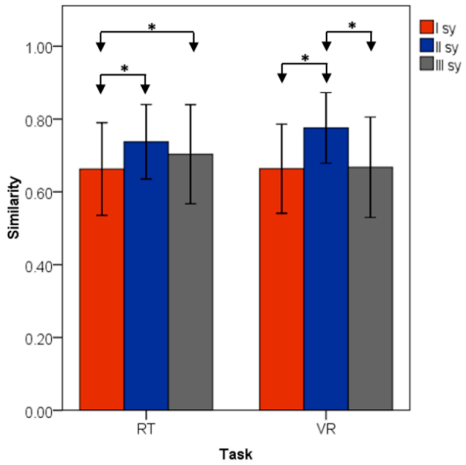

Figure 6. Mean value and standard deviation of cos_{sim} for the between-subject analysis. RT and VR stand for real task and virtual reality, respectively. * indicates statistical differences.

4. Discussion

The present study sought to evaluate changes in muscle synergy organization based on throwing tasks in healthy young subjects, when performed in a virtual reality environment. Differences between real and virtual throwing gestures were calculated by comparing the number of muscle synergies and by analyzing the similarity of their inner composition. In addition, the role of dominant and nondominant arm was investigated, as well as the inter-subject similarity of the muscle synergy vectors.

The range of selected muscle synergies across the examined subjects, i.e., 2–5, and the mode value equal to 3 confirms the ability of the CNS to reduce the complexity of muscle organization in performing physical activities [29,42,53]. In particular, the most likely value found in this study is in line with a previous study focused on throwing tasks [54], thereby demonstrating that a three-synergy model is sufficient to describe the activation of the trunk and upper limb muscles during overhead throws in healthy, young subjects.

By analyzing the results of the statistical analysis on NoS, we can conclude that the execution of the overhead throws, in a virtual reality environment, does not cause a variation in the number of muscle synergies enrolled when performing the task. As a further confirmation, cosine similarity analyses showed that the weights related to the *i*-th synergy and to the overall model are highly similar between virtual and real throws, when considering the dominant and nondominant arm.

This finding indicates that there is no significant difference in the neuromuscular organization of virtual reality throws and real ones, thereby suggesting that healthy subjects are able to activate the same muscles with a similar timing despite the absence of a real object to grab. Therefore, when the subjects launched a virtual ball, their neuromuscular organization is no different from the one adopted when clutching a real one, as well as in terms of activating the muscles that control hand grasping. As depicted in Figure 5, synergy weights related to the forearm muscles, i.e., #5 and #6, are significantly involved, suggesting activation of the muscles during the execution of the task. This indicates that VR tasks are able to elicit activation of muscles involved in an already-known real-life gesture, even when generation of muscle force is not needed. The importance of this specific finding to the field of rehabilitation is not minor, considering that the forearm muscles are the ones mostly involved for the execution of daily life activity and, consequently, their rehabilitation is fundamental after upper limb injuries [55].

Similar outcomes were reported by Kang et al. [28], who showed similar activity of upper limb muscles in performing both virtual and actual archery motions. Moreover, the equal benefits of virtual reality, in terms of physical recovery in traditional clinical practices, have already been demonstrated in several clinical applications, such as training a patient with neurological diseases

[56] to turn while walking, increasing the endurance of the pelvic floor muscle in postmenopausal women [57], recovering upper limb movements in poststroke patients [58], and improving the smoothness of movement in children with cerebral palsy [59].

From this perspective, our results allow us to consider virtual reality as a viable tool for rehabilitation programs related to the recovery of muscle control and as an alternative to traditional therapies. It is worth noting that a virtual reality approach is characterized by several advantages compared to a traditional one [60]. Firstly, it has been accepted that serious games implemented in a VR environment increase patient engagement and simplify complex tasks [6]. Secondly, virtual reality guarantees the adaptability and variability of programs tailored to the patient's needs [58]. Thirdly, it is also possible to quantify patient performance and store the subject's data for remote access [61]. Finally, the use of VR in home-based rehabilitation can help to reduce the medical costs [61]. Thus, considering the aforementioned results, the effects of physical treatment can also be simulated by the motion activities performed in a VR environment. Additionally, this approach could be useful for coaching when designing suitable training programs in sports, where overhead throws are fundamental gestures; this includes baseball, volleyball, javelin throws, and so on [62].

However, we should also consider that a more complete VR, as opposed to conventional therapy/training, is still questionable; Laver et al. suggested that the benefits of VR in improving upper limb functionality when performing physical tasks may occur when used as an adjunct to traditional methods and was used to increase the overall therapy/training time [63].

When comparing the dominant and nondominant upper limb, a highly similar muscle synergy organization was observed when performing both the virtual and real throws. Similar results were also observed in the muscle activation of healthy subjects in reaching tasks [64], in handgrip strength to grip a basketball [65], and in force and angular velocity related to the arm in baseball pitchers [66]. Conversely, difference in kinematics were noted in the dominant arm during the throwing tasks; specifically, the nondominant arm was characterized by significantly lower elbow flexion and in the external shoulder rotation at the start of the arm acceleration phase [67]. These findings suggest that a virtual task leads to a variation in the kinematics of the subject's adaptation to a different environment, while motor control remains similar and is only related to the activation level. Considering our findings and those already published in the literature, we can state that if the rehabilitation/training program is focused on the recovery of muscle activity, there is no requirement that it be tailored to the dominant arm. Conversely, a specific program should be designed if kinematic improvement is to be achieved.

Concerning the inter-subject similarity, the three-synergy model revealed itself as consistent across different subjects, both considering the *i*-th synergy and the overall model. As previously mentioned, this synergy model is in line with the one shown by Cruz-Ruiz et al. [54]. Then, by observing the inner composition of the muscle synergy model, a specific role can be assigned to each synergy in the model when considering the biomechanics of the overhead throws [68]. More specifically, a throw can be partitioned into three main phases: (i) arm cocking, which is the movement performed until the maximum shoulder rotation; (ii) arm acceleration, which is from the maximum shoulder external rotation until ball release; and (iii) arm deceleration, which is from the ball release until the arm stops internally rotating. Thus, considering the muscles involved, the first synergy in the model is consistent with the biomechanical actions needed during the cocking phase, especially when enrolling trapezius and deltoideus and FCU and BB for the grip of the ball. The second and third synergies, instead, primarily include muscles that are involved during the deceleration and acceleration phase, respectively.

These findings suggest that healthy subjects are characterized by similar muscle activation patterns, especially in the deceleration phase, considering the statistical differences found for the $\cos_{sim}$ value related to the second synergy. This result can be ascribed to the absence of specific expertise of our subjects during overhead throws. In fact, it has already been verified that arm cocking and arm acceleration are primarily responsible for improved throwing [69]; thus, it is conceivable that these two phases are more variable in nonexpert subjects.

5. Conclusions

In this paper, we have analyzed the effects of virtual reality on muscle synergies in throwing tasks performed with both dominant and nondominant arms. In addition, inter-subject similarities were assessed. The outcomes of our study endorse virtual reality as a valuable tool for rehabilitation/training programs that focus on muscle recovery, since a very high similarity was found in a real throwing task. No differences were found between dominant and nondominant arms, and a three-synergy model can be considered consistent across subjects when describing the muscle activity in overhead throwing. Future work will include the combination of EMG outputs with kinematic ones to enable a more in-depth analysis of the throwing motion.

Author Contributions: Conceptualization, E.S., J.T., D.R.H., Z.D.P., S.R. and E.P.; Data curation, E.S., J.T., D.R.H. and E.P.; Methodology, E.S., J.T., S.R. and E.P.; Project administration, E.S., J.T., D.R.H., Z.D.P., S.R. and E.P.; Supervision, J.T., Z.D.P., S.R. and E.P.; Writing—original draft, E.S., J.T. and E.P.; Writing—review & editing, E.S., J.T., D.R.H., Z.D.P., S.R. and E.P.

Funding: This research received no external funding.

Conflicts of Interest: The authors declare no conflict of interest.

References

1. Sisto, S.A.; Forrest, G.F.; Glendinning, D. Virtual Reality Applications for Motor Rehabilitation After Stroke. *Top. Stroke Rehabil.* **2002**, *8*, 11–23.
2. Desai, P.R.; Desai, P.N.; Ajmera, K.D.; Mehta, K. A Review Paper on Oculus Rift-A Virtual Reality Headset. *Int. J. Eng. Trands Technol.* **2014**, *13*, 175–179.
3. Connelly, L.; Yicheng Jia; Toro, M.L.; Stoykov, M.E.; Kenyon, R. V.; Kamper, D.G. A Pneumatic Glove and Immersive Virtual Reality Environment for Hand Rehabilitative Training After Stroke. *IEEE Trans. Neural Syst. Rehabil. Eng.* **2010**, *18*, 551–559.
4. Freina, L.; Ott, M. *A Literature Review on Immersive Virtual Reality in Education*; State of the Art and Perspectives: New York, NY, USA, 2015.
5. Schultheis, M.T.; Rizzo, A.A. The application of virtual reality technology in rehabilitation. *Rehabil. Psychol.* **2001**, *46*, 296.
6. Ma, M.; Zheng, H. Virtual Reality and Serious Games in Healthcare. In *Advanced Computational Intelligence Paradigms in Healthcare 6. Virtual Reality in Psychotherapy, Rehabilitation, and Assessment*; Springer: Berlin/Heidelberg, Germany, 2011; pp. 169–192.
7. Feigin, V.; Forouzanfar, M.; Krishnamurthi, R.; Mensah, G.; Connor, M.; Bennet, D.; Moran, A.; Sacco, R.; Anderson, L.; Truelsen, T.; et al. Global and regional burden of stroke during 1990–2010: Findings from the Global Burden of Disease Study 2010. *Lancet* **2014**, *383*, 245–54.
8. Colombo, R.; Sterpi, I.; Mazzone, A.; Delconte, C.; Pisano, F. Robot-aided neurorehabilitation in sub-acute and chronic stroke: Does spontaneous recovery have a limited impact on outcome? *NeuroRehabilitation* **2013**, *33*, 621–629.
9. Schaechter, J.D. Motor rehabilitation and brain plasticity after hemiparetic stroke. *Prog. Neurobiol.* **2004**, *73*, 61–72.
10. Taub, E.; Uswatte, G.; Mark, V.W.; Morris, D.M.; Barman, J.; Bowman, M.H.; Bryson, C.; Delgado, A.; Bishop-McKay, S. Method for Enhancing Real-World Use of a More Affected Arm in Chronic Stroke: Transfer Package of Constraint-Induced Movement Therapy. *Stroke* **2013**, *44*, 1383–1388.
11. Cappa, P.; Clerico, A.; Nov, O.; Porfiri, M. Can force feedback and science learning enhance the effectiveness of neuro-rehabilitation? An experimental study on using a low-cost 3D joystick and a virtual visit to a zoo. *PLoS ONE* **2013**, *8*, e83945.
12. Summa, S.; Basteris, A.; Betti, E.; Sanguineti, V. Adaptive training with full-body movements to reduce bradykinesia in persons with Parkinson's disease: A pilot study. *J. Neuroeng. Rehabil.* **2015**, *12*, 16.
13. Kwakkel, G.; Kollen, B.J.; Krebs, H.I. Effects of robot-assisted therapy on upper limb recovery after stroke: A systematic review. *Neurorehabil. Neural Repair* **2007**, *22*, 111–121.
14. Chang, C.; Chang, Y.; Chang, H.; Chou, L. An interactive game-based shoulder wheel system for rehabilitation. *Patient Prefer. Adher.* **2012**, *6*, 821–828.

15. Cheok, G.; Tan, D.; Low, A.; Hewitt, J. Is Nintendo Wii an Effective Intervention for Individuals With Stroke? A Systematic Review and Meta-Analysis. *J. Am. Med. Dir. Assoc.* **2015**, *16*, 923–932.
16. Huang, H.; Wolf, S.L.; He, J. Recent developments in biofeedback for neuromotor rehabilitation. *J. Neuroeng. Rehabil.* **2006**, *3*, 1–12.
17. Scalona, E.; Martelli, F.; Del Prete, Z.; Palermo, E.; Rossi, S. A Novel Protocol for the Evaluation of Motor Learning in 3D Reching Tasks Using Novint Falcon. In Proceedings of the 7th IEEE International Conference on Biomedical Robotics and Biomechatronics (Biorob), Overijssel, The Netherlands, 26–29 August 2018; pp. 268–272.
18. Pastor, I.; Hayes, H.; Bamberg, S. A feasibility study of an upper limb rehabilitation system using kinect and computer games. *Conf. Proc. IEEE Eng. Med. Biol. Soc.* **2012**, *2012*, 1286–1289.
19. Laut, J.; Cappa, F.; Nov, O.; Porfiri, M. Increasing Patient Engagement in Rehabilitation Exercises Using Computer-Based Citizen Science. *PLoS ONE* **2015**, *10*, e0117013.
20. Scalona, E.; Hayes, D.; Del Prete, Z.; Palermo, E.; Rossi, S. Perturbed Point-to-Point Reaching Tasks in a 3D Environment Using a Portable Haptic Device. *Electronics* **2019**, *8*, 32.
21. Chang, Y.-J.; Chen, S.-F.; Huang, J.-D. A Kinect-based system for physical rehabilitation: A pilot study for young adults with motor disabilities. *Res. Dev. Disabil.* **2011**, *32*, 2566–2570.
22. Webster, D.; Celik, O. Systematic review of Kinect applications in elderly care and stroke rehabilitation. *J. Neuroeng. Rehabil.* **2014**, *11*, 108–111.
23. Lange, B.; Chang, C.Y.; Suma, E.; Newman, B.; Rizzo, A.S.; Bolas, M. Development and evaluation of low cost game-based balance rehabilitation tool using the Microsoft Kinect sensor. In Proceedings of the IEEE Engineering in Medicine and Biology Conference, Boston, MA, USA, 30 August–03 September 2011.
24. Mitra, S.; Acharya, T. Gesture recognition: A survey. *IEEE Trans. Syst. Man Cybern.* **2007**, *37*, 311–324.
25. Hondori, H.M.; Khademi, M. A review on technical and clinical impact of microsoft kinect on physical therapy and rehabilitation. *J. Med. Eng.* **2014**, *2014*, 1–16.
26. Palermo, E.; Laut, J.; Nov, O.; Cappa, P.; Porfiri, M. A Natural User Interface to Integrate Citizen Science and Physical Exercise. *PLoS ONE* **2017**, *12*, e0172587, 1–21.
27. Sabatini, A. Identification of neuromuscular synergies in natural upper-arm movements. *Biol. Cybern.* **2002**, *86*, 253–262.
28. Kang, J.H.; Park, T.S. Analysis of Muscle On-set Time of Fully Immersive Virtual Reality Motions and Actual Motions in Healthy Adults. *Int. J. Pure Appl. Math.* **2018**, *118*, 2367–2380.
29. Bizzi, E.; Cheung, V.C.K.; d'Avella, A.; Saltiel, P.; Tresch, M. Combining modules for movement. *Brain Res. Rev.* **2008**, *57*, 125–133.
30. Tresch, M.C. Matrix Factorization Algorithms for the Identification of Muscle Synergies: Evaluation on Simulated and Experimental Data Sets. *J. Neurophysiol.* **2005**, *95*, 2199–212.
31. Neptune, R.R.; Clark, D.J.; Kautz, S.A. Modular control of human walking: A simulation study. *J. Biomech.* **2009**, *42*, 1282–1287.
32. Santuz, A.; Ekizos, A.; Janshen, L.; Baltzopoulos, V.; Arampatzis, A. on the Methodological Implications of Extracting Muscle Synergies From Human Locomotion. *Int. J. Neural Syst.* **2016**, *27*, 1–15.
33. Ivanenko, Y.P.; Poppele, R.E.; Lacquaniti, F. Five basic muscle activation patterns account for muscle activity during human locomotion. *J. Physiol.* **2004**, *1*, 267–282.
34. Taborri, J.; Palermo, E.; Masiello, D.; Rossi, S. Factorization of EMG via muscle synergies in walking task: Evaluation of intra-subject and inter-subject variability. In Proceedings of the IEEE International Instrumentation and Measurement Technology Conference, Torino, Italy, 22–25 May 2017.
35. Ting, L.H.; Macpherson, J.M. A Limited Set of Muscle Synergies for Force Control During a Postural Task. *J. Neurophysiol.* **2005**, *93*, 609–613.
36. Taborri, J.; Mileti, I.; Del Prete, Z.; Rossi, S.; Palermo, E. Yaw Postural Perturbation Through Robotic Platform: Aging Effects on Muscle Synergies. In Proceedings of the 7th IEEE International Conference on Biomedical Robotics and Biomechatronics (Biorob), Overijssel, The Netherlands, 26–29 August 2018; pp. 916–921.
37. Torres-oviedo, G.; Ting, L.H. Subject-Specific Muscle Synergies in Human Balance Control Are Consistent Across Different Biomechanical Contexts. *J. Neurophysiol.* **2010**, *103*, 3084–3098.
38. Taborri, J.; Agostini, V.; Artemiadis, P.K.; Ghislieri, M.; Jacobs, D.A.; Roh, J.; Rossi, S. Feasibility of muscle synergy outcomes in clinics, robotics, and sports: A systematic review. *Appl. Bionics Biomech.* **2018**, *2018*, 1–19.

39. Zelik, K.E.; Scaleia, V. La; Ivanenko, Y.P.; Lacquaniti, F. Can modular strategies simplify neural control of multidirectional human locomotion? *J. Neurophysiol.* **2014**, *111*, 1686–1702.
40. Lacquaniti, F.; Ivanenko, Y.P.; Zago, M. Patterned control of human locomotion. *J. Physiol.* **2012**, *590*, 2189–2199.
41. Rosevall, J.; Rusu, C.; Talavera, G.; Carrabina, J.; Garcia, J.; Carenas, C.; Breuil, F.; Reixach, E.; Torrent, M.; Burkard, S.; et al. A wireless sensor insole for collecting gait data. *Stud. Heal. Technol. Inf.* **2014**, *200*, 176–178.
42. Taborri, J.; Palermo, E.; Prete, Z. Del; Rossi, S. On the reliability and repeatability of surface electromyography factorization by muscle synergies in daily life activities. *Appl. Bionics Biomech.* **2018**, *2018*, 1–15.
43. Rau, G.; Disselhorst-Klug, C.; Biomechanics, R.S.-J. of; 2000, U. Movement biomechanics goes upwards: From the leg to the arm. *J. Biomech.* **2000**, *33*, 1207–1216.
44. Cruz Ruiz, A.L.; Pontonnier, C.; Levy, J.; Dumont, G. Motion Control via Muscle Synergies: Application to Throwing. In Proceedings of the 8th International ACM SIGGRAPH Conference on Motion in Games 2015 (MIG'15), Paris, France, 16–18 November 2015.
45. Stegeman, D.F.; Hermens, H.J. Standards for Surface Electromyography: The European Project Surface EMG for Non-Invasive Assessment of Muscles (SENIAM). Available online: http//www.med.uni-jena.de/motorik/pdf/stegeman.pdf (accessed on day month year).
46. Scalona, E.; Taborri, J.; Del Prete, Z.; Palermo, E.; Rossi, S. EMG factorization during walking: Does digital filtering influence the accuracy in the evaluation of the muscle synergy number? In Proceedings of the 2018 IEEE International Symposium on Medical Measurements and Applications (MeMeA), Rome, Italy, 11–13 June 2018; pp. 1–6.
47. Lee, D.D.; Seung, H.S. Learning the parts of objects by non-negative matrix factorization. *Nature* **2000**, *401*, 788–791.
48. Shuman, B.; Goudriaan, M.; Bar-on, L.; Schwartz, M.H.; Desloovere, K.; Steele, K.M. Repeatability of muscle synergies within and between days for typically developing children and children with cerebral palsy. *Gait Posture* **2016**, *45*, 127–132.
49. Field, A. *Discovering Statistics Using SPSS*, 3rd ed.; Sage Publications Ltd.: Newbury Park, CA, USA, 2013; ISBN 978-184-787-9066.
50. Hug, F.; Turpin, N.A.; Guével, A.; Dorel, S. Is interindividual variability of EMG patterns in trained cyclists related to different muscle synergies? *J. Appl. Physiol.* **2010**, *108*, 1727–1736.
51. Spath, H. *Helmuth The Cluster Dissection and Analysis Theory FORTRAN Programs Examples*; Prentice-Hall, Inc.: Upper Saddle River, NJ, USA, 1985; ISBN 013-137-9852.
52. D'Avella, A.; Saltiel, P.; Bizzi, E. Combinations of muscle synergies in the construction of a natural motor behavior. *Nat. Neurosci.* **2003**, *6*, 300–308.
53. Chvatal, S.A.; Ting, L.H. Common muscle synergies for balance and walking. *Front. Comput. Neurosci.* **2013**, *7*, 1–14.
54. Cruz Ruiz, A.L.; Pontonnier, C.; Sorel, A.; Dumont, G. Identifying representative muscle synergies in overhead football throws. *Comput. Methods Biomech. Biomed. Eng.* **2015**, *18*, 1918–1919.
55. Padilla-Castañeda, M.A.; Sotgiu, E.; Barsotti, M.; Frisoli, A.; Orsini, P.; Martiradonna, A.; Laddaga, C.; Bergamasco, M. An Orthopaedic Robotic-Assisted Rehabilitation Method of the Forearm in Virtual Reality Physiotherapy. *J. Healthc. Eng.* **2018**, *2018*, 1–20.
56. Oh, K.; Stanley, C.J.; Damiano, D.L.; Kim, J.; Yoon, J.; Park, H.S. Biomechanical evaluation of virtual reality-based turning on a self-paced linear treadmill. *Gait Posture* **2018**, *65*, 157–162.
57. Martinho, N.; Carvalho, L.C.; Iunes, D.H.; Botelho, S.; Marques, J.; Silva, V.R. The effects of training by virtual reality or gym ball on pelvic floor muscle strength in postmenopausal women: a randomized controlled trial. *Braz. J. Phys. Ther.* **2016**, *20*, 248–257.
58. Aşkın, A.; Atar, E.; Koçyiğit, H.; Tosun, A. Effects of Kinect-based virtual reality game training on upper extremity motor recovery in chronic stroke. *Somatosens. Mot. Res.* **2018**, *35*, 25–32.
59. McNish, R.N.; Chembrammel, P.; Speidel, N.C.; Lin, J.J.; López-Ortiz, C. Rehabilitation for children with dystonic cerebral palsy using haptic feedback in virtual reality: Protocol for a randomized controlled trial. *J. Med. Internet Res.* **2019**, *21*, 1–13.
60. Sveistrup, H. Motor rehabilitation using virtual reality. *J. Neuroeng. Rehabil.* **2004**, *1*, 1–8.
61. Burdea, G.C. Virtual Rehabilitation—Benefits and Challenges. *Methods Inf. Med.* **2003**, *42*, 519–523.

62. Hermassi, S.; van den Tillaar, R.; Khlifa, R.; Chelly, M.S.; Chamari, K. Comparison of In-Season-Specific Resistance vs. A Regular Throwing Training Program on Throwing Velocity, Anthropometry, and Power Performance in Elite Handball Players. *J. Strength Cond. Res.* **2015**, *29*, 2105–2114.
63. Laver, K.E.; George, S.; Crotty, M.; Lange, B.; Deutsch, J.E.; Saposnik, G. Virtual reality for stroke rehabilitation. *Cochrane Database Syst. Rev.* **2017**, *11*, 1–4.
64. Peters, K.M.; Kelly, V.E.; Chang, T.; Weismann, M.C.; Westcott McCoy, S.; Steele, K.M. Muscle recruitment and coordination during upper-extremity functional tests. *J. Electromyogr. Kinesiol.* **2018**, *38*, 143–150.
65. Priya, S.; Rai, M.; Joseph, D.M. Comparison between Handgrip Strength Measurement of Dominant Hand and Non Dominant Hand in Basketball Players. *Indian J. Physiother. Occup. Ther.* **2018**, *12*, 126–130.
66. Escamilla, R.F.; Fleisig, G.S.; Zheng, N.; Barrentine, S.W.; Andrews, J.R. Kinematic comparisons of 1996 Olympic baseball pitchers. *J. Sports Sci.* **2001**, *19*, 665–676.
67. Sachlikidis, A.; Salter, C. A biomechanical comparison of dominant and non-dominant arm throws for speed and accuracy. *Sports Biomech.* **2007**, *6*, 334–344.
68. Wilk, K.E.; Meister, K.; Fleisig, G.; Andrews, J.R. Biomechanics of the Overhead Throwing Motion. *Sports Med. Arthrosc.* **2000**, *8*, 124–134.
69. Baltaci, G.; Tunay, V.B. Isokinetic performance at diagonal pattern and shoulder mobility in elite overhead athletes. *Scand. J. Med. Sci. Sports* **2004**, *14*, 231–238.